

ENERGY DISSIPATION MECHANISMS IN WAVE BREAKING PROCESSES

A. Iafrati, INSEAN-CNR (Italian Ship Model Basin-National Research Council), Rome, Italy,
E-mail: a.iafrati@insean.it

SUMMARY

The mechanisms governing the energy dissipation in wave breaking processes are investigated numerically by a two-fluid numerical model. The flow is assumed two-dimensional and both air and water are considered as incompressible. Simulations are carried out for periodic wave trains with different initial amplitude. Attention is devoted to two cases in which the wave train evolves toward a spilling and a plunging breaking event. The analysis covers: velocity and vorticity field, work done against pressure forces, viscous dissipation and bubbles dynamics. It is shown that in gentle spilling case, dissipation is mostly due to the viscous effects in the shear layer generated by the interaction between the fluid in bulge and the flow underneath. This effect dissipates all the extra-energy and progressively recondacts the wave to the highest non-breaking solution. In the plunging breaking case, the rather important role played by the entrainment of the large air cavity at the breaking onset is highlighted. Results show that the work is initially spent in entraining the air cavity against the bouyancy. In the next stage the cavity fragments into a cloud of small bubbles immersed in a highly rotational flow and large velocity gradients. Most of the potential energy accumulated by the air cavity is thus dissipated in the bubble cloud by the strong viscous effects, whereas only a little amount is returned to water in the degassing phase.

1. INTRODUCTION

The breaking of free surface waves plays an important role on many exchange processes at the air-sea interface. In wind generated waves in open ocean, the breaking governs the mixing in the upper ocean layer but it also has a strong effect of the wind-wave interaction. Detailed, non-intrusive, experimental investigation of the above phenomena are not always easy. This is particularly true in intense plunging breaking where the light reflection from the large bubbles make it hard to use optical instruments (Particle Image or Laser Doppler Velocimetry). Measurements are presently available only for times $t > t_b + 3T$ where t_b is the time of breaking onset and T is the period of the fundamental wave. Something more is available for gentle spilling breaking (Duncan, 2001; Qiao and Duncan, 2001), but a more quantitative analysis in terms of energy dissipation would be necessary.

In the present paper, a two-fluid numerical approach is adopted to model the air-water interaction taking place in wave breaking processes. The method is applied to study the evolution to breaking of periodic wave trains of different initial amplitude. The details of the model and of the simulation parameters are discussed in Iafrati (2009a) and some results concerning the degassing phase were presented at the Workshop in Saint Petersburg (Iafrati, 2009b). Here, the attention is focussed on two breaking cases, i.e. a gentle spilling and a plunging. The solutions are analysed in detail in order to highlights the different dissipation mechanisms.

2. NUMERICAL MODEL

For the sake of the space, only few key points of the method are discussed here whereas a more detailed description of the model can be found in Iafrati (2009a). The method is based on a Navier-Stokes solver for a single, incompressible, fluid whose density and viscosity vary smoothly across a small transition region about the interface. The transition region is about ten grid cells thick. Surface tension effects are appropriately modelled as a volume force acting in the same

region. Simulations are carried out within a two dimensional assumption.

The interface is captured as the zero Level-Set of a signed distance function d from the interface which is advected with the flow, thus ensuring that particles lying on the free surface at the beginning of the step keep the same value of the distance $d = 0$. The distance function is reinitialized at each time step in order to keep constant in space and time the thickness of the transition region, thus avoiding an excessive spreading of the interface.

The method is adopted to simulate the evolution to breaking of periodic wave trains in a computational domain with periodic boundary conditions. The solution is initialized as a third order Stokes wave and the initial amplitude is varied so that the initial steepness ranges between 0.2 and 0.65. Attention is here focussed on the solutions obtained for 0.35 and 0.60 for which a gentle spilling and an intensive plugging breaking are obtained, respectively.

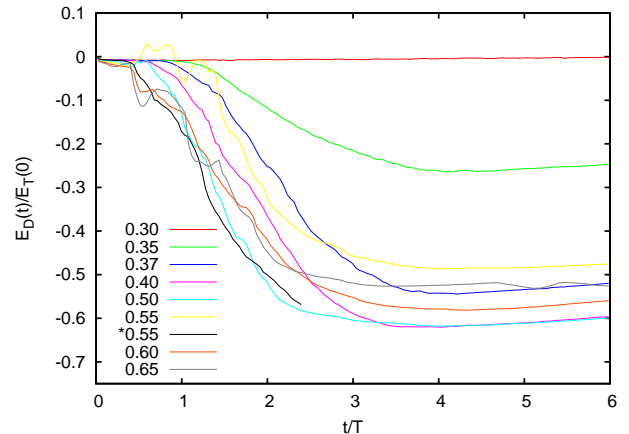


Figure 1: Time histories of the energy dissipated by the breaking scaled by the initial energy content in water. For the case at $\varepsilon = 0.55$ the solution at two different Reynolds number are drawn.

3. ENERGY DISSIPATED BY BREAKING

It is well accepted that the occurrence of breaking significantly enhances the dissipation of the initial energy content. In order to get a quantitative estimate of the energy portion dissipated by the breaking occurrence it is necessary to estimate the energy that would be dissipated in the same time interval if the wave hadn't broke.

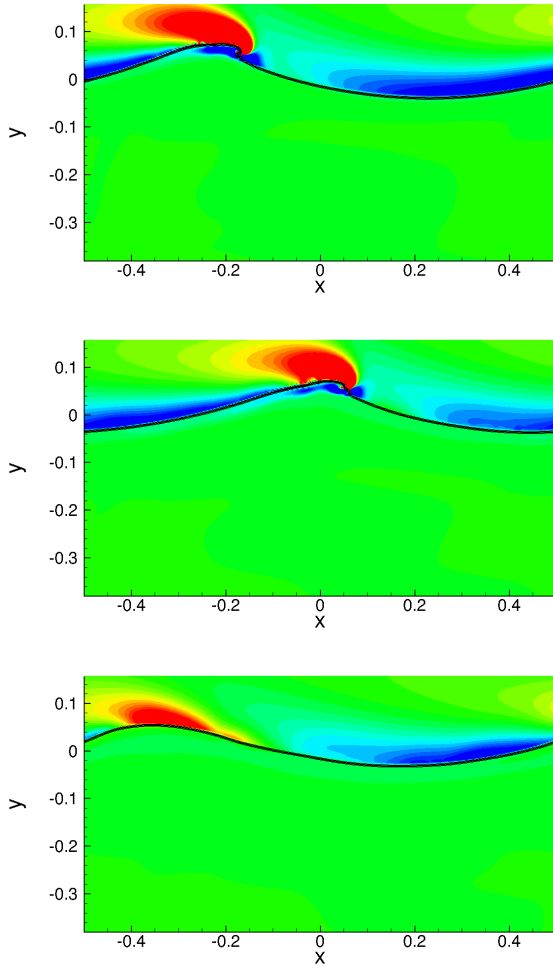


Figure 2: Vorticity contours at different time instants for the case $\varepsilon = 0.35$ ($t/T = 1.596, 2.713, 5.186$).

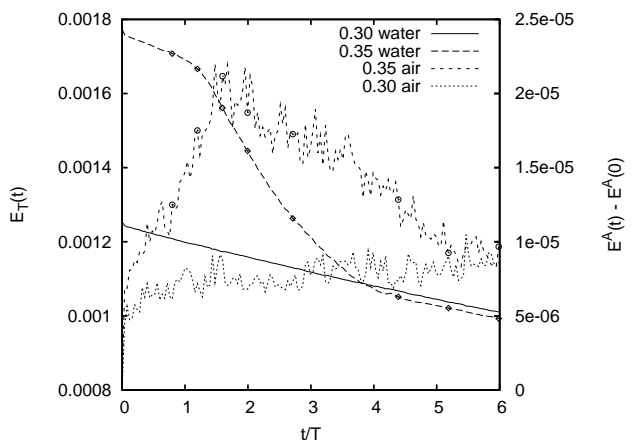


Figure 3: Time histories of the total energy (left axis) and of the energy accumulated in air (right axis) for the steepest non-breaking solution ($\varepsilon = 0.30$) and for the spilling breaking case.

This is done by using the theoretical estimate of the energy decay rate derived in Landau and Lipshitz (1959) for a sinusoidal wave. Hence, the energy dissipated by the breaking at a given time $E_D(t)$ is evaluated as the difference between the total energy in water (including kinetic, potential and surface tension) and the energy that would be dissipated by a regular wave with the same amplitude and wavelength.

In Fig. 1 the time histories of the energy dissipated by the breaking occurrence are drawn for different steepness. In order to make results comparable, solutions are scaled by the corresponding initial energy contents. For the configuration adopted in this study, the spilling breaking case dissipates a fraction of about 25 % of the initial energy content. The fraction rise up to 60 % in the plunging breaking case. It is worth noticing that in the plunging breaking regime the energy fraction dissipated by the breaking is almost independent of the breaking severity. In all cases, most of the energy is dissipated within 3 fundamental wave periods from the onset of breaking (in the present result the breaking starts for $t/T \simeq 0.5 \div 1$ depending on the wave amplitude).

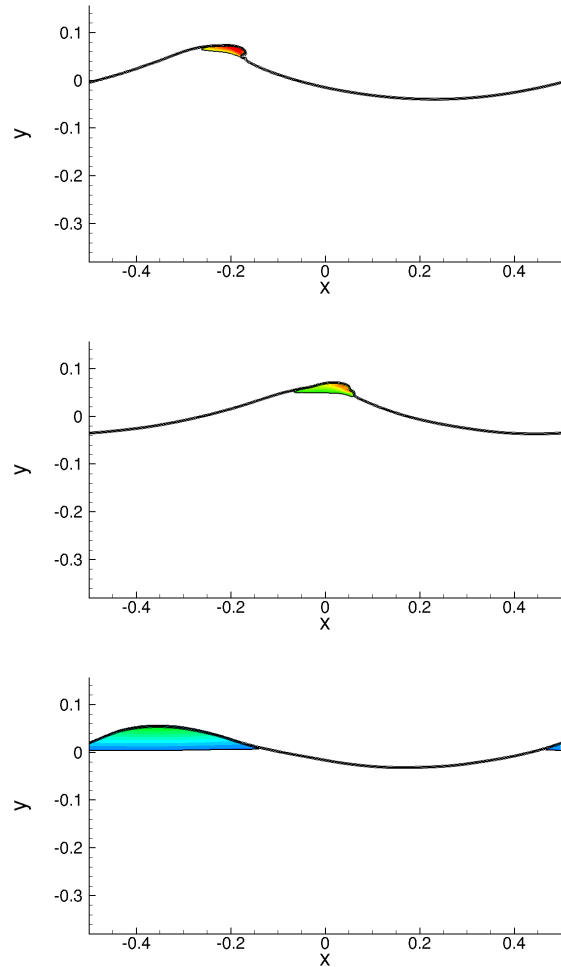


Figure 4: Contours of the local energy density for the case $\varepsilon = 0.35$ ($t/T = 1.596, 2.713, 5.186$).

4. SPILLING BREAKING CASE

At $\varepsilon = 0.35$ and for the scale adopted in the simulations, $We=100$ or 27 cm fundamental wavelength, the breaking takes place with the formation of a bulge at the wave crest. A shear layer develops between the fluid inside the bulge and the upslope flow underneath (Fig. 2). This shear layer gradually dissipates the extra-energy and drives the solution toward that of the highest non-breaking case. Similar conclusions can be drawn by looking at the comparison in terms of the non-scaled total energy provided in Fig. 3, where the solution obtained for $\varepsilon = 0.30$ (i.e. the steepest non-breaking case among the available solutions) are also drawn. Results indicate that in this gentle spilling breaking case the energy is gradually dissipated until it reaches the energy of the almost steepest non-breaking case. The figure also indicates that the occurrence of breaking enhances the energy transfer in air, but this transfer is only a negligible fraction, order of 2.5 %, of the total energy dissipation.

Interesting conclusions can be drawn by looking at the distribution of the energy density in the water domain. In the three pictures in Fig. 4 the contours of the energy density are drawn in the top 90 % region, i.e. where the local energy density E_d is greater than $E_d^{90} = \sup E_d - 0.1(\sup E_d - \inf E_d)$. The sequence indicates that the largest energy density is localized inside the bulge.

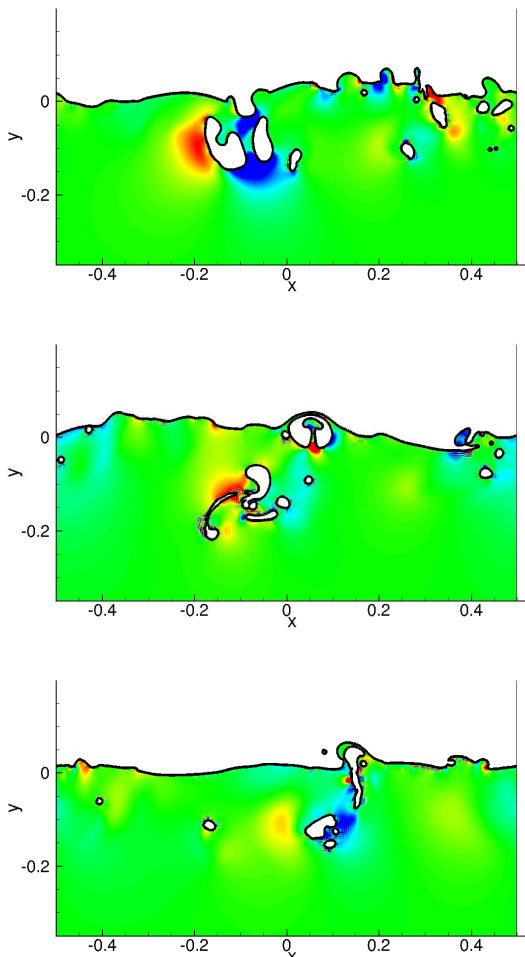


Figure 5: Contours of the work done against pressure forces, $-\nabla(pu)$. Solution refer to the case $\varepsilon = 0.60$ ($t/T = 1.596, 1.995, 2.394$).

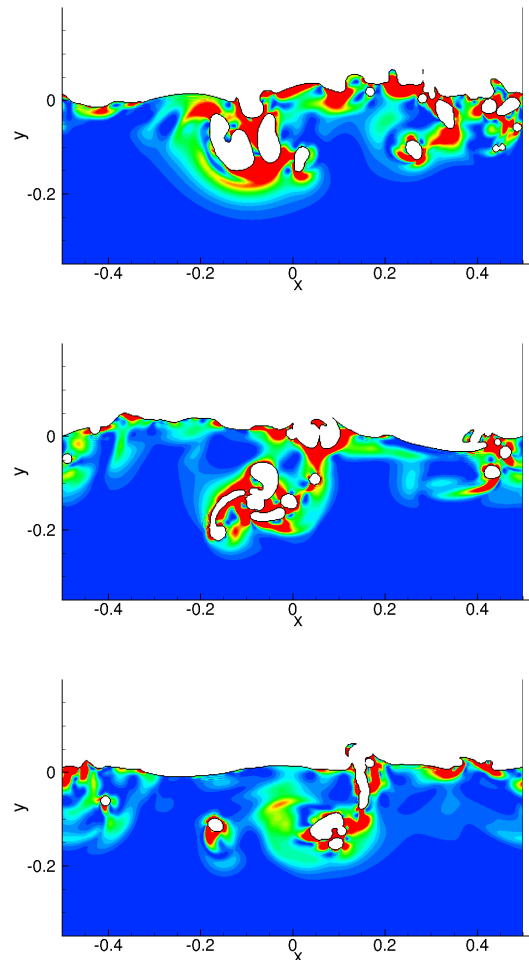


Figure 6: Contours the viscous dissipation in the pure water domain. The configurations refer to the same time instant of Fig. 5.

Quantitative estimates showed that, for the first two pictures in Fig. 4, a fraction between 10 to 14 % of the energy content in water is within the bulge. In the late stage (Fig. 4c), once all the extra-energy is dissipated, the distribution of the energy resembles that of non-breaking wave (not shown here).

5. PLUNGING BREAKING CASE

When the steepness is beyond $\varepsilon = 0.37$, the breaking is of the plunging type. In this case the energy fraction dissipated by the breaking is much larger and can rise up to 60 % of the initial energy content. In this case the jet encompasses a large air cavity which is advected downward. A large amount of energy is spent in entraining the air cavity against the action of buoyancy. Unfortunately, the use of a smooth density variation introduces a spurious velocity component which make it difficult to get accurate estimates of the momentum exchanges and of the work done by the stresses at the interface.

A qualitative estimate of the phenomenon can be achieved by looking at the distribution of the term $-\nabla(pu)$, which is the work done against pressure forces. The configurations shown in Fig. 5 highlights the negative effect associated to the downward advection of the air cavity. In the next stage the potential energy accumulated by the air cavity should

be returned to water. However, the air cavity collapse and fragments into a clouds of small bubbles immersed in a rotating flow with large velocity gradients. As a consequence, most of the potential energy of the bubbles is dissipated by the viscous effects. This is clearly shown by the pictures in Fig. 6 where the contours of the viscous dissipation in pure water domain are provided.

From the quantitative standpoint, in Fig. 7 the time histories are shown for: energy dissipated by the breaking, energy accumulated in air, surface tension energy and potential energy in the bubbles. Among other considerations that can be drawn, it can be seen that the potential energy accumulated in the bubble in the most energetic phase of the breaking rise up to about 50 % of the total energy dissipated by the breaking occurrence. This result agrees with the experimental observation by Lamarre and Melville (1991).

A more extensive discussion, with additional results, will be presented at the Workshop.

6. REFERENCES

J.H. Duncan (2001) *Spilling breakers*, Ann. Rev. Fluid Mech., 33, 519-547.

A. Iafrati (2009a) *Numerical study of the effects of the breaking intensity on wave breaking flows*, J. Fluid Mech., 622, 371-411.

A. Iafrati (2009b) *Air entrainment and degassing process in breaking waves*, 24th IWWF, Saint Petersburg.

E. Lamarre and W.K. Melville (1991) *Air entrainment and dissipation in breaking waves*, Nature, 351, 469-472.

L.D. Landau and E.M. Lifshitz (1959), Fluid Mechanics, Pergamon.

H. Qiao and J.H. Duncan (2001) *Gentle spilling breakers: crest flow-field evolution*, J. Fluid Mech., 439, 57-85.

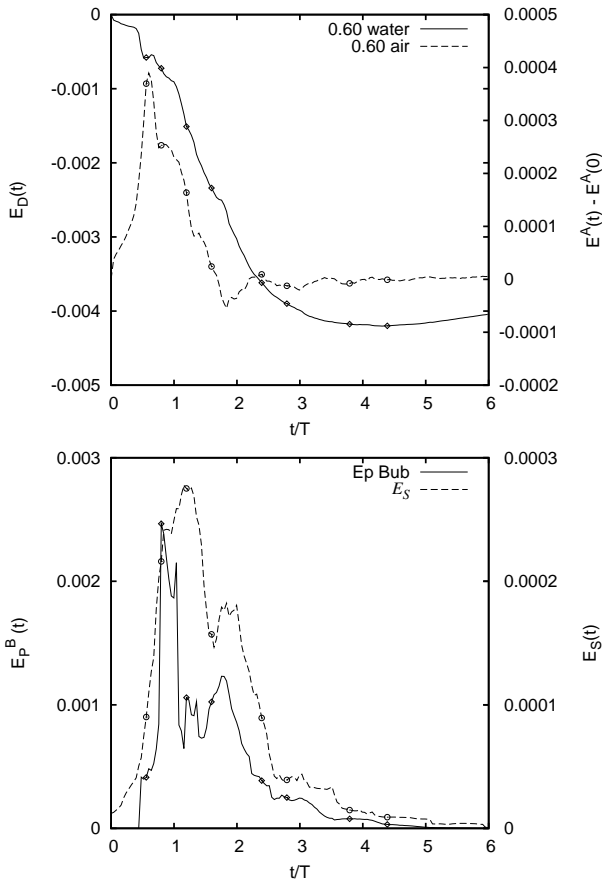


Figure 7: On top, time histories of the energy dissipated by the breaking $E_D(t)$ (left axis) and of the energy accumulated in air $E_A(t) - E_A(0)$ (right axis) for the case $\epsilon = 0.60$. On the bottom figure, time histories of the potential energy of the bubbles (left axis) and of the surface tension energy (right axis) for the same simulation.